

Unitary equilibration after a quantum quench of a thermal state

N. Tobias Jacobson,^{1,*} Lorenzo Campos Venuti,² and Paolo Zanardi^{1,2}

¹*Department of Physics and Astronomy and Center for Quantum Information Science & Technology,
University of Southern California, Los Angeles, California 90089-0484, USA*

²*Institute for Scientific Interchange (ISI), Viale S. Severo 65, I-10133 Torino, Italy*

In this work we investigate the equilibration dynamics after a sudden Hamiltonian quench of a quantum spin system initially prepared in a thermal state. To characterize the equilibration we evaluate the Loschmidt echo, a global measure for the degree of distinguishability between the initial and time-evolved quenched states. We present general results valid for small quenches and detailed analysis of the quantum XY chain. The result is that quantum criticality manifests, even at small but finite temperatures, in a universal double-peaked form of the echo statistics and poor equilibration for sufficiently relevant perturbations. In addition, for this model we find a tight lower bound on the Loschmidt echo in terms of the purity of the initial state and the more-easily-evaluated Hilbert-Schmidt inner product between initial and time-evolved quenched states. This bound allows us to relate the time-averaged Loschmidt echo with the purity of the time-averaged state, a quantity that has been shown to provide an upper bound on the variance of observables.

PACS numbers:

I. INTRODUCTION

Consider a finite and isolated system initialized to a stationary state of a Hamiltonian H_0 . The system is then instantaneously quenched and left to evolve unitarily according to a Hamiltonian H_1 [1–4]. If we wait a sufficiently long time, will this system ever equilibrate? It turns out that strong equilibration cannot occur through unitary dynamics, since no asymptotic stationary state can be reached from a non-stationary initial state. System observables may equilibrate in a *probabilistic* sense, however, in that for the vast majority of time observable expectations remain near to their time-averaged values. Beginning more than eighty years ago [5] and with resurgent interest in recent years, a great deal of attention has been devoted to characterizing the equilibration dynamics of such a system with the goal of deriving from first principles the emergence of statistical mechanics [6–13].

In this paper, we investigate the effect that proximity to quantum criticality has on the equilibration dynamics after a quench for the realistic situation of finite temperature. To quantify the equilibration behavior we compute the Loschmidt echo (LE), a measure for the degree of distinguishability between initial and time-evolved quenched states that has been used to study phenomena such as quantum chaos [14–16], decoherence [17–21], and quantum criticality [19, 22–24]. In [23, 24], general arguments have been given, for systems at zero temperature, that quenching near a quantum critical point leads to poor equilibration and a universal double-peaked distribution for observables. More recently, in Ref. [25] we have shown that, even at finite temperature, the infinite-time probability distribution of the Loschmidt echo takes one of two universal forms, either double-peaked or Log-Normal. Here we will explore this behavior in more detail. In addition, we find a tight lower bound for the Loschmidt echo of this model in terms of a linearized quantity that permits comparison of

the time-averaged Loschmidt echo with recent results in the statistical mechanics literature.

This paper is organized as follows: in Sec. II we introduce in general terms the problem of equilibration for unitarily-evolving systems. In Sec. III we discuss the Loschmidt echo for thermal states in the general case and for small quenches in particular. In Sec. IV we move to consider the free fermion case and introduce the Linearized Loschmidt Echo and related bounds. In Sec. V we analyze in detail the XY chain and its Ising and anisotropy transitions. Finally, Sec. VI contains the conclusions and the appendices detail several calculations omitted in the main text.

II. UNITARY EQUILIBRATION

Under open quantum dynamics, it can occur that the system relaxes towards an equilibrium state and remains near to it for (almost) all times [26]. However, under unitary dynamics this kind of strong equilibration cannot happen, except for the trivial case where the initial state is stationary. The absence of strong equilibration can be seen clearly through the following argument. At time t the state of the system is given by $\rho(t) = U(t)\rho(0)U^\dagger(t)$, with $U(t)$ the unitary quantum evolution. If $\rho(t)$ had a limit, say $\rho(\infty)$, for $t \rightarrow \infty$, this limit must coincide with its time-average $\bar{\rho} := \lim_{\tau \rightarrow \infty} \tau^{-1} \int_0^\tau \rho(t) dt$. On the other hand, the invariance of $\bar{\rho}$ under the dynamics, i.e. $U(s)\bar{\rho}U^\dagger(s) = \bar{\rho}$, implies that $\|\rho(t) - \rho(\infty)\| = \|\rho(t) - \bar{\rho}\| = \|\rho(0) - \bar{\rho}\|$ is constant for any unitary-invariant norm $\|\cdot\|$ (for example, the trace norm). But then one cannot have $\lim_{t \rightarrow \infty} \|\rho(t) - \rho(\infty)\| = 0$ unless $\rho(t) = \rho(0) = \bar{\rho}$, in which case the dynamics is trivial. This argument shows that, in the general case $\rho(t)$ cannot have a limit in the strong sense, i.e. in norm. However, a weaker form of equilibration may occur, namely the equilibration of observables in a probabilistic sense. More precisely, we say that an observable A equilibrates in a system specified by initial condition $\rho(0)$ and unitary evolution $U(t)$, if the expectation value $\langle A(t) \rangle := \text{tr}(\rho(t)A)$ stays close to its

*Electronic address: ntj@usc.edu

“equilibrium value” for most of the times t in the observation interval $[0, \tau]$. Since the observation time is generally much larger than the microscopic time-scales of the dynamics, it is customary to take the limit $\tau \rightarrow \infty$. One way to check the condition for equilibration as given above is to consider the probability distribution $P_A(a) := \overline{\delta(\langle A(t) \rangle - a)}$. $P_A(a) da$ gives the probability of observing a value $\langle A(t) \rangle$ in the interval $[a, a + da]$, during the time interval $[0, \tau]$ (and taking the limit $\tau \rightarrow \infty$). Concentration results for $P_A(a)$, i.e. results indicating the peakedness of $P_A(a)$, correspond to good equilibration. Roughly speaking, in order to show concentration results for $P_A(a)$, one needs to have access to higher and higher moments or ideally the whole distribution. The first moment, the average value of an observable, is given in terms of the “equilibrium” state $\bar{\rho}$: $\langle A(t) \rangle = \text{tr}(\bar{\rho}A)$.

P. Reimann [9] found that the variance of an observable can be upper-bounded in terms of the purity of the time-averaged equilibrium state $\bar{\rho}$:

$$\sigma_A^2 \leq \Delta_A^2 \text{Tr}[\bar{\rho}^2], \quad (1)$$

where $\sigma_A^2 = \overline{(\text{Tr}[A\rho(t)] - \text{Tr}[A\bar{\rho}])^2}$ is the variance of the expectation of A and the *range* of A , Δ_A , is a measure of the size of the observable (more precisely, Δ_A is the spread of the expectations of A : $\Delta_A = (a_{\max} - a_{\min})$, with respect to states in the support of the initial state $\rho(0)$ [9]). As we can see, small purity of the equilibrium state implies small variance for all observables within a given range, and hence equilibration for a wide class of observables.

III. THE LOSCHMIDT ECHO

Given a system prepared in some initial equilibrium state ρ of a Hamiltonian H_0 , we would like to characterize the time-dependent degree of distinguishability between this state and the time-evolved states arising from the action of another Hamiltonian H_1 on ρ . The quantity we consider is the Loschmidt echo, given by

$$\mathcal{L}(t) = F(\rho(t), \rho(0)). \quad (2)$$

Here F is the Uhlmann fidelity $F(\rho, \sigma) = (\text{Tr} \sqrt{\rho^{\frac{1}{2}} \sigma \rho^{\frac{1}{2}}})^2$, which characterizes the degree of distinguishability between two mixed states [27]. In this work we call H_0 (H_1) the pre (post)-quench Hamiltonian, and take the initial state and Hamiltonian to commute, $[H_0, \rho] = 0$.

Note that the convention we take here is to square the trace, while in some works the Loschmidt echo is defined without the square [28]. With our convention, if ρ and σ are pure states the Uhlmann fidelity is equivalent to a transition probability rather than a transition amplitude. Moreover, if either (or both) of ρ and σ are pure states, then the Uhlmann fidelity simplifies to $F(\rho, \sigma) = \text{Tr}[\rho\sigma]$. In particular, if the initial state is an eigenstate of the initial Hamiltonian, $\rho = |\Psi_0\rangle\langle\Psi_0|$, then the Loschmidt echo reduces to $\mathcal{L}(t) = |\langle\Psi_0|e^{-itH_1}|\Psi_0\rangle|^2$, also known as the “survival probability” in this case.

The Loschmidt echo (2) can be equivalently expressed in terms of a trace norm, $\mathcal{L}(t) = \|\rho^{\frac{1}{2}}\rho(t)^{\frac{1}{2}}\|_F^2$, where $\|A\|_1 \equiv$

$\text{Tr}|A| = \text{Tr}(\sqrt{A^\dagger A})$. Replacing $\|\cdot\|_1$ with the Frobenius norm $\|\cdot\|_F$ ($\|A\|_F = \sqrt{\text{Tr}[A^\dagger A]}$), one obtains a simpler “linearized” form of the Loschmidt echo

$$\mathcal{L}_F(t) := \|\rho^{\frac{1}{2}}\rho(t)^{\frac{1}{2}}\|_F^2 = \text{Tr}(\rho(t)\rho) \leq \mathcal{L}(t), \quad (3)$$

where the bound above follows from $\|A\|_F \leq \|A\|_1$. Note that this linearized quantity is generally much more convenient to evaluate than the true Loschmidt echo, owing to the absence of the square-roots appearing in the Uhlmann fidelity.

The aforementioned bound always holds, but we will later find a significantly tighter lower bound on the Loschmidt echo for our model which is otherwise valid in general only for single-qubit states (see Appendices A and B).

A. Statistics for generic Hamiltonians

We are interested in the equilibration properties of the Loschmidt echo over long times. As reminded above, although the Loschmidt echo is a purely deterministic quantity, it is useful to treat it as a random variable in order for statistical methods to be brought to bear. That is, we take the LE as a random variable given by its value at a random time t chosen uniformly from an interval $t \in [0, \tau]$, and then take the limit $\tau \rightarrow \infty$. In numerical simulations (such as the ones reported here) τ is necessarily finite. In order to reproduce correctly the $\tau \rightarrow \infty$ limit, at least as far as the first moments are concerned, a safe estimate is to take $\tau \gg (\min_{m,n}(E_m - E_n))^{-1}$, which can be as large as an exponential of the system size. This turns out to be a far too restrictive requirement, and for the case of quasi-free fermions analyzed here, we verified that taking $\tau \propto L^2$ is sufficient in order to have reliable distributions, in the sense that larger τ produce similar distributions (see also the discussion in Sec. II C of Ref. [23]). We thus consider the LE probability distribution $P_{\mathcal{L}}(x) := \overline{\delta(\mathcal{L}(t) - x)}$, the full-time statistics. We are interested in studying $P_{\mathcal{L}}(x)$ as the temperature and quench parameters are varied.

In the case of a pure initial state, the first moment of P i.e. the time-averaged Loschmidt echo, equals the purity of the time-averaged state: $\overline{\mathcal{L}} = \text{Tr}[\bar{\rho}^2]$. Hence from Eq (1) it follows that for this case a smaller $\overline{\mathcal{L}}$ corresponds to a smaller variance (1) for generic observables and hence “good” quantum equilibration. However, in the case we are considering here where the initial state can be mixed, we will see that the LE need not be small for the equilibrium purity to be small.

In Ref. [25], we found that the LE takes one of two universal forms, either Log-Normal in the off-critical region or double-peaked in the quasi-critical region. That is, considering the variable $\mathcal{Z}(t) := \ln \mathcal{L}(t)$, the distribution for the *logarithm* of the LE, $P_{\mathcal{Z}}(x)$ is then correspondingly either Gaussian or double-peaked. We obtained this result for a quasi-free system through a central limit theorem (CLT)-type argument for \mathcal{Z} . In Ref. [25], we also argued that such universal statistics should hold as well for small quenches with generic (i.e. not necessarily quasi-free) Hamiltonians in the pure case, i.e. at zero temperature.

B. Small quenches

We now provide an argument in favor of the preceding result also in the mixed, i.e. non-zero temperature, case. Namely, for small quenches of generic Hamiltonians and thermal initial states proximity to quantum criticality gives rise to double-peaked statistics, whereas otherwise, in the off-critical region, one expects Gaussian behavior for $P_{\mathcal{Z}}(x)$.

Suppose our post-quench Hamiltonian is $H_1 = \sum_n E_n^1 |\psi_n\rangle\langle\psi_n|$ and our initial state is given by $\rho(0) = \sum_{n,m} \rho_{n,m} |\psi_n\rangle\langle\psi_m|$. We assume that this state is diagonal in the pre-quench Hamiltonian's eigenbasis, $\rho(0) = \sum_n p_n |n\rangle\langle n|$, where we take $\{|n\rangle\}$ ($\{|\psi_n\rangle\}$) to correspond to the pre (post)-quench Hamiltonian eigenstates. For nearby states $\rho, \rho + \delta\rho$, the lowest-order expansion of the Uhlmann fidelity is given by [29, 30]

$$F(\rho, \rho + \delta\rho) = 1 - \frac{1}{2} \sum_{m,n} \frac{|\langle m|\delta\rho|n\rangle|^2}{p_m + p_n}. \quad (4)$$

In our case $\delta\rho$ will be time-dependent and correspond to the difference between $\rho(t)$ and $\rho(0)$. In order to use the expansion Eq. (4), we have to show that $\delta\rho(t)$ is small in V *independently* of t , since we will use such an expansion for any time t . To see this, compute $\delta\rho(t)$ exactly in the post-quench eigenbasis:

$$\begin{aligned} \delta\rho(t) &= \rho(t) - \rho(0) \\ &= \sum_{n \neq m} \rho_{n,m} \left(e^{-it(E_n^1 - E_m^1)} - 1 \right) |\psi_n\rangle\langle\psi_m|. \end{aligned} \quad (5)$$

Observe that $\delta\rho(t)$ has only off-diagonal elements in the post-quench basis. Now using time-independent perturbation theory (and assuming a non-degenerate spectrum for simplicity), one can show that for $n \neq m$, $|\rho_{n,m}| \leq \text{const.} \times V$ (where for simplicity of notation V denotes also the strength of the perturbation). By then bounding the time-oscillating terms by two, we obtain $\|\delta\rho(t)\| \leq O(V)$ in some norm, independent of t . This argument indicates that one can use a Dyson expansion for any arbitrary time t .

Evaluating the matrix element $\langle m|\delta\rho(t)|n\rangle$ up to first order in the perturbation using Eqs. (4) and (5) we obtain, to second order in the perturbation

$$\mathcal{L}(t) \simeq 1 - \sum_{n \neq m} C_{n,m} [1 - \cos[(E_m^1 - E_n^1)t]], \quad (6)$$

where

$$C_{n,m} = \frac{(p_m - p_n)^2}{p_m + p_n} \frac{|V_{m,n}|^2}{(E_m^0 - E_n^0)^2} \quad (7)$$

and $V_{m,n} = \langle m|V|n\rangle$. We can now take the time-average of Eq. (6) with any arbitrarily-large observation time τ (i.e. also $\tau \rightarrow \infty$), with the result that the time-averaged Loschmidt echo is given by

$$\bar{\mathcal{L}} = 1 - \sum_{n \neq m} \frac{(p_m - p_n)^2}{p_m + p_n} \frac{|V_{m,n}|^2}{(E_m^0 - E_n^0)^2}. \quad (8)$$

We next show how this time-average is related with the state fidelity. Let us then consider, in general, the Uhlmann fidelity $F(\rho_0, \rho_1)$ between two nearby states $\rho_0, \rho_1 = \rho_0 + \delta\rho$. For example, ρ_0 (ρ_1) can be a thermal Gibbs state relative to the pre (post)-quench Hamiltonian H_0 (H_1). For small quenches $\delta\rho = O(V)$ and we can use the general expansion Eq. (4) which defines the Bures distance ds^2 . The variation $\delta\rho$ in this case takes contributions both from the change of eigenvalues and eigenvectors, $\delta\rho = \sum_n (d\rho_n |n\rangle\langle n| + p_n (|dn\rangle\langle n| + |n\rangle\langle dn|))$. Differentiating the eigenvalue equation $H|n\rangle = E_n|n\rangle$ in order to evaluate $\langle m|dn\rangle$, we obtain [31]

$$\begin{aligned} F &= 1 - ds^2 \\ ds^2 &= \frac{1}{4} ds_{\text{FR}}^2 + \frac{1}{2} \sum_{n \neq m} \frac{(p_m - p_n)^2}{p_m + p_n} \frac{|\langle m|dH|n\rangle|^2}{(E_n - E_m)^2}. \end{aligned} \quad (9)$$

Here ds^2 is the Bures metric, while ds_{FR}^2 is the so-called Fisher-Rao distance between probability distributions corresponding to the sets of diagonal weights $\{p_n\}$ and $\{p_n + dp_n\}$ and is given by $ds_{\text{FR}}^2 = \sum_n dp_n^2/p_n$. The second term in Eq. (9) is what is denoted the ‘‘non-classical’’ part and depends on the variation of the eigenstates [31]. Through comparing Eqns. (9) and (8), we can establish the relation $[F(\rho_0, \rho_1)]^2 = \bar{\mathcal{L}} - ds_{\text{FR}}^2/2$, valid up to second order in the perturbation. This result provides a relation between the Loschmidt echo (a dynamical quantity) and the state fidelity (a static one). For pure initial states (when the ‘‘temperature’’ goes to zero) one recovers $F^2 = \bar{\mathcal{L}}$ [17], since in this limit the classical part of the Bures metric which depends on the variation of the eigenvalues vanishes [31].

Let us now analyze the full time statistics and consider the logarithm of the Loschmidt echo for small quenches, Eq. (6). Assuming the initial state is of the Gibbs form $\rho(0) = e^{-\beta H_0}/Z$, the weights p_n are given by $p_n = e^{-\beta E_n^0}/Z$. This means that the largest weights $C_{n,m}$ are to be found when either n or m is zero, since $C_{n,m} \ll C_{n,0}$ for all $m \neq 0$, a result which is (exponentially) stronger the lower the temperature. For temperatures sufficiently low as compared to the gaps, i.e. $\beta(E_1^0 - E_0^0) \gg 1$, a good approximation to $\ln \mathcal{L}(t)$ is then given by (taking $W_{n,m} = 2C_{n,m}$)

$$\mathcal{Z}(t) \simeq \bar{\mathcal{Z}} + \sum_{n>0} W_{n,0} \cos((E_n^0 - E_0^0)t), \quad (10)$$

with $\bar{\mathcal{Z}} = -\sum_{n \neq m} C_{n,m}$.

If we now assume that the perturbed energy gaps $\Delta_n := (E_n^0 - E_0^0)$ are *rationally independent* (i.e. linearly independent over the field of rational numbers), using the ergodic theorem one realizes that $\mathcal{Z}(t) - \bar{\mathcal{Z}}$ is a *sum of independent* random variables each distributed according to $P(z_n) = \vartheta(W_{n,0}^2 - z_n^2) / (\pi \sqrt{W_{n,0}^2 - z_n^2})$ [25]. To see this let us compute the characteristic function of the variable $\mathcal{Z} - \bar{\mathcal{Z}}$, $e^{i\lambda(\mathcal{Z} - \bar{\mathcal{Z}})}$. Rational independence allows to invoke the ergodic theorem and to compute the time expectation value as an average over a multidimensional torus with uniform mea-

sure:

$$\overline{e^{i\lambda(\mathcal{Z}-\bar{\mathcal{Z}})}} = \prod_{n>0} \int_0^{2\pi} \frac{d\vartheta_n}{2\pi} e^{i\lambda W_{n,0} \cos(\vartheta_n)}. \quad (11)$$

This also shows that \mathcal{Z} is a sum of independent variables since the characteristic function factorizes into a product of functions. The integration over each angle gives a Bessel function $J_0(|\lambda W_{n,0}|)$. The probability distribution of each mode is computed by Fourier transforming this Bessel function and gives rise to the distribution $P(z_n)$ given above. Each $P(z_n)$ is the density of states (DOS) of a one-dimensional tight-binding model with coupling $W_{n,0}/2$ and has mean zero and variance given by $(W_{n,0})^2/2$. The collective distribution of $\mathcal{Z}(t) - \bar{\mathcal{Z}}$ is also given, in principle, by the DOS of a huge-dimensional ($D - 1$, where D is the Hilbert space dimension) tight-binding model with anisotropic couplings $W_{n,0}/2$ in each direction. Given that the size of D is large, the distribution of \mathcal{Z} is better computed using a central limit theorem-type argument. Therefore we need to control the weights $W_{n,0}$ which determine the variance of \mathcal{Z} .

C. Temperature and criticality

The weights $W_{n,0}$ are simply temperature-damped versions of their corresponding $T = 0$ values: $W_{n,0}(T) = \mathcal{D}_n(T) W_{n,0}(T = 0)$, where

$$\mathcal{D}_n(T) = \frac{e^{-\beta E_0^0} (e^{-\beta \Delta_n} - 1)^2}{Z} \frac{1}{e^{-\beta \Delta_n} + 1}$$

and $W_{n,0}(0) = 2|V_{n,0}|^2/(E_n^0 - E_0^0)^2$. The temperature damping factor $0 \leq \mathcal{D}_n(T) \leq 1$ has simply the effect of attenuating the level n as temperature increases.

Let us first review the situation at $T = 0$. The factor $W_{n,0}(0)$ has already been considered in [24, 25, 32, 33]. It was found that close to quantum criticality, $W_{n,0}$ scales with the energy as $E^{-2/(\zeta\nu)}$, where ζ is the dynamical critical exponent and ν is the correlation length one. The algebraic divergence at low energy of $W_{n,0}(0)$ has the effect that, sufficiently close to criticality (i.e. when the correlation length ξ is much larger than the linear system size L), few low-energy weights $W_{n,0}(0)$ absorb most of the total weight [24]. In turn this implies that, at $T = 0$, the sum over n in Eq. (10) can be safely restricted to a small number n_{\max} of energy levels. As a result, the distribution of \mathcal{Z} is the DOS of an n_{\max} -dimensional tight-binding model. For small n_{\max} (i.e. $n_{\max} \leq 2 \div 3$) such a distribution is a double-peaked function with a large variance [23, 24] corresponding to a universal kind of poor equilibration.

We can now ask ourselves how this result will be modified when switching on the temperature $T > 0$. If $\Delta(\xi)$ denotes the energy gap above the ground state (correlation length) one has to consider different cases

- a) Region I: $\xi \gg L < \infty$ and $\Delta \ll T = \beta^{-1}$ (in any case the temperature must still be sufficiently small with respect to the energy scale of the problem). The condition

$\Delta/T \ll 1$ allows to expand the temperature-damping factor $\mathcal{D}_n(T)$ as $\mathcal{D}_n(T) \simeq E^2/T^2$. Combining this result with the zero-temperature scaling we obtain

$$W_n(T) \simeq E^{2-2/(\zeta\nu)}/T^2$$

The divergence observed at zero temperature is softened by the factor E^2 , but there still may be situations where $W_n(T)$ diverges at low energy, namely for $\zeta\nu < 1$. In other words, in the quasi-critical region the possibility of observing a double-peaked distribution for \mathcal{Z} depends on the relevance of the perturbation. For sufficiently relevant perturbation, $\zeta\nu < 1$ (or differently put $\Delta_V < d$, where d is the spatial dimension and Δ_V the scaling dimension of V) the distribution of \mathcal{Z} is double-peaked, whereas for $\zeta\nu \geq 1$ the expected behavior is the Gaussian one corresponding to ‘‘good’’ equilibration.

- b) Region II: $\xi \gg L$ but $\Delta \gg T$. The condition $\Delta/T \gg 1$ fixes $\mathcal{D}_n(T)$ to one up to exponentially small corrections, and we recover the $T = 0$ case, namely a double-peaked distribution for \mathcal{Z} corresponding to poor equilibration.
- c) Region III (off-critical region, thermodynamic limit): $L \gg \xi$. The variance of \mathcal{Z} is given by $\kappa_2(\mathcal{Z}) = (1/2) \sum_n [W_{n,0}(T)]^2$. For a sufficiently small perturbation both $\mathcal{D}_n(T)$ and $W_{n,0}(0)$ will be between zero and one. Then

$$2\kappa_2(\mathcal{Z}) \leq \sum_n [W_{n,0}(0)]^2 \leq \sum_n W_{n,0}(0) \equiv \chi_F$$

The quantity χ_F is the (zero-temperature) ‘‘fidelity susceptibility’’ and was shown to grow at most extensively in the off-critical region [34]. Hence $\kappa_2(\mathcal{Z}) \leq O(L)$ and the rescaled variable $\mathcal{Y} := (\mathcal{Z} - \bar{\mathcal{Z}})/\sqrt{L}$ tends in distribution, as $L \rightarrow \infty$, to a Gaussian with zero mean and variance $\sigma^2 = \lim_{L \rightarrow \infty} \kappa_2(\mathcal{Z})/L$ (the limit exists because $\kappa_2(\mathcal{Z})$ is monotonically increasing with L , since \mathcal{Z} is a sum of independent variables).

- d) Finally, for the sake of completeness, we analyze the high-temperature region. For $\Delta_n/T \ll 1$ ($\forall n$) one has $\mathcal{D}_n(T) = O(T^{-2})$ and therefore $\mathcal{L}(t) = 1 - O(T^{-2})$. This is of course just a consequence of the fact that the thermal state approaches the maximally mixed one for infinite temperature and the latter has trivial dynamics (for all Hamiltonians).

IV. QUASI-FREE FERMIONS

We now turn our attention to a special class of systems for which a closed-form expression for the Loschmidt echo has been found [22]: those systems described by a quasi-free fermion Hamiltonian

$$H = \sum_k \epsilon_k (c_k^\dagger c_k + c_{-k}^\dagger c_{-k}) + \Delta_k (-i c_k^\dagger c_{-k}^\dagger + i c_{-k} c_k), \quad (12)$$

where c_k^\dagger (c_k) create (annihilate) spinless fermions. Such a model can be recast in a diagonal form $H = \sum_k \Lambda_k \eta_k^\dagger \eta_k$, where $\{\Lambda_k\}$ are single-particle energies. Imposing anti-periodic boundary conditions, the quasi-momenta k are quantized according to $k = (2n+1)\pi/L$, where $n = 0, \dots, L-1$ and we will assume L to be even.

The Gibbs (thermal) state of such a model at inverse temperature β takes the form of a tensor-product of 4×4 density matrices [22],

$$\rho = \frac{e^{-\beta H}}{Z} = \bigotimes_{k>0} \frac{1}{Z_k} \left(\rho_k^{\text{even}} \oplus \mathbb{I}_k^{\text{odd}} \right), \quad (13)$$

where ρ_k^{even} is a 2×2 matrix over the ‘‘even’’ subspace spanned by $\{|0\rangle, c_k^\dagger c_{-k}^\dagger |0\rangle\}$ and $\mathbb{I}_k^{\text{odd}}$ is the 2×2 identity operator over the ‘‘odd’’ subspace $\{c_k^\dagger |0\rangle, c_{-k}^\dagger |0\rangle\}$. The tensor product is over $L/2$ momentum modes. This splitting of a given momentum mode into an even and odd subspace is a consequence of the Hamiltonian acting only trivially (as an energy shift) on the odd subspace [22].

For any quench Hamiltonian H of the form (12) the unitary operator $U(t) = e^{-itH}$ is directly analogous to (13), as can be seen readily by performing a Wick rotation $\beta \rightarrow it$.

Exploiting the special factorized form of the Gibbs state and the evolution operator, we are able to prove the following bound (see Appendix B).

$$\frac{\text{Tr}(U\rho U^\dagger \rho)}{\text{Tr}(\rho^2)} \leq \left(\text{Tr} \sqrt{\rho^{\frac{1}{2}} U \rho U^\dagger \rho^{\frac{1}{2}}} \right)^2. \quad (14)$$

This inequality provides a much-tighter lower bound on the Loschmidt echo than the general inequality (3). Note that $U \rightarrow \mathbb{I}$ gives unity on both sides of the inequality. The inverse purity is usually given the name of *effective dimension*, $d_{\text{eff}} := 1/\text{Tr}(\rho^2)$ [10]. The effective dimension provides a weighted measure of how broadly the ensemble weights of ρ are distributed [10]. In particular, the effective dimension of a pure state is unity while that of a maximally-mixed state is equal to the Hilbert space dimension. Inequality (14) may then be expressed equivalently as

$$d_{\text{eff}} \mathcal{L}_F(t) \leq \mathcal{L}(t). \quad (15)$$

The tightness of this bound with respect to (3) can be appreciated since $1 \leq d_{\text{eff}} \leq d$, where d is the Hilbert space dimension. Again, we stress that (15) is not generally applicable to states belonging to a Hilbert space of dimension greater than two. We remark that the quantity on the left-hand side of inequality (15) was proposed by Peres in Ref. [14] as a generalization of the Loschmidt echo to mixed states.

To bound $\mathcal{L}(t)$ from above we employ the following generally-applicable inequality in terms of the so-called *super-fidelity* due to Mischczak, et al. [28]

$$\text{Tr} \left[\sqrt{\rho^{\frac{1}{2}} \sigma \rho^{\frac{1}{2}}} \right]^2 \leq \text{Tr}[\rho\sigma] + \sqrt{(1 - \text{Tr}\rho^2)(1 - \text{Tr}\sigma^2)}. \quad (16)$$

Putting this all together, we can now bound the Loschmidt echo from below and above in terms of the linearized echo:

$$d_{\text{eff}} \mathcal{L}_F(t) \leq \mathcal{L}(t) \leq \mathcal{L}_F(t) + \left(1 - d_{\text{eff}}^{-1}\right). \quad (17)$$

Observe that these bounds become tighter as the purity of the initial state gets closer to unity. This corresponds, in our setting, to the low-temperature regime. Note that for $t = 0$ the upper and lower bounds are equal, so by continuity they are expected to characterize well the short-time behavior of $\mathcal{L}(t)$. Typical behavior of $\mathcal{L}(t)$ and $d_{\text{eff}} \mathcal{L}_F(t)$ is depicted in Fig. 1. The Loschmidt echo drops from unity at $t = 0$ and then oscillates about its average value, with almost periodic revivals [35]. We find that, at each fixed time, \mathcal{L} monotonically increases with temperature, which can be understood as being due to the Gibbs state tending towards the totally-mixed state \mathbb{I}/d for increasing temperature.

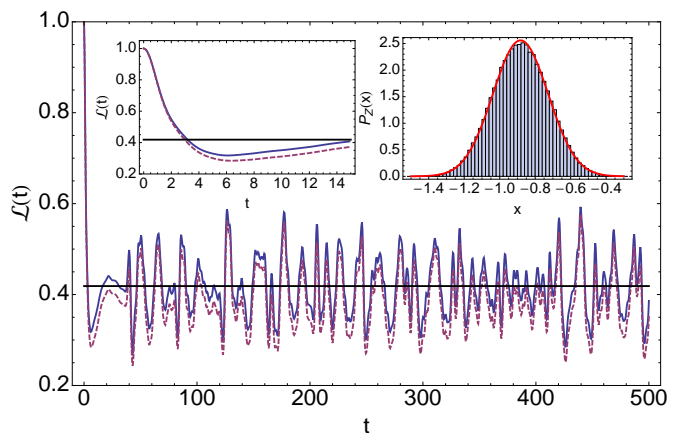


Figure 1: (Color online) Time series of $\mathcal{L}(t)$ (solid) and $d_{\text{eff}} \mathcal{L}_F(t)$ (dashed) along with the average $\bar{\mathcal{L}}$ for the quantum XY chain, with $L = 80$, $h^{0,1} = 0.5$, $\gamma^0 = 0.25$, $\gamma^1 = 0.1$ and $\beta = 10$. In the left inset the initial Gaussian decay is evident. The right inset shows a histogram of $\mathcal{Z} = \ln \mathcal{L}$ with a superimposed Gaussian distribution (red) of the same mean and variance.

A. Loschmidt Echo Statistics

For model (12), the Loschmidt echo has been shown to be [22]

$$\mathcal{L}(t) = \prod_{k>0} \left[\frac{1 + \sqrt{c_k^2 - (c_k^2 - 1)\alpha_k \sin^2(\Lambda_k^1 t)}}{1 + c_k} \right]^2, \quad (18)$$

where $c_k = \cosh(\beta \Lambda_k^0)$, $\alpha_k = \sin^2(\Delta\theta_k)$, $\Delta\theta_k = \theta_k^1 - \theta_k^0$, and $\theta_k = \arctan(\Delta_k/\epsilon_k)$.

The linearized LE and the effective dimension have similar, though simpler, product forms (see Appendices D and C):

$$\mathcal{L}_F(t) = d_{\text{eff}}^{-1} \prod_{k>0} [1 - (1 - c_k^{-2})\alpha_k \sin^2(\Lambda_k^1 t)] \quad (19)$$

and

$$d_{\text{eff}}^{-1} = \text{Tr} [\rho^2] = \prod_{k>0} [c_k / (c_k + 1)]^2. \quad (20)$$

Since c_k increases monotonically with the temperature, the effective dimension ranges continuously and monotonically, from $d_{\text{eff}} = 1$ at $T = 0$ to $d_{\text{eff}} = d$, the Hilbert space dimension, when $T \rightarrow \infty$.

The time average of (18) is (see Appendix E):

$$\overline{\mathcal{L}} = \prod_{k>0} \left[1 - (1 - c_k^{-1}) \frac{\alpha_k}{2} + g_k \right], \quad (21)$$

where $g_k \equiv \frac{2c_k}{(1+c_k)^2} \left[\frac{2}{\pi} \text{E}(-b_k) - \frac{b_k}{4} - 1 \right]$ and $\text{E}(x)$ is the complete elliptic integral.

The time-averaged linearized echo, $\overline{\mathcal{L}_F(t)} = \text{Tr} [\overline{\rho(t)}\rho]$, is easier to evaluate. Assuming rational independence of half of the single-particle energies, $\{\Lambda_k\}_{k>0}$ [41], the time-average is

$$\overline{\mathcal{L}_F(t)} = d_{\text{eff}}^{-1} \prod_{k>0} \left[1 - (1 - c_k^{-2}) \frac{\alpha_k}{2} \right]. \quad (22)$$

As we can see in Eq. (22), to obtain a smaller $\overline{\mathcal{L}_F}$ we can either increase the effective dimension (by increasing the temperature, for example) or enhance the strength of the quench.

Note that the equilibrium state $\overline{\rho}$ is diagonal in the eigenbasis of the quench Hamiltonian. To see this, expand the initial state in terms of the quench Hamiltonian eigenbasis and take the time average, exploiting the non-degeneracy of the spectrum (see e.g. [10]). The equilibrium state is then only the diagonal part of the initial state in the quench basis. Consequently,

$$\overline{\mathcal{L}_F(t)} = \text{Tr} [\overline{\rho}^2], \quad (23)$$

i.e. the time-averaged linearized echo is simply the purity of the equilibrium state. Plugging this into the inequality (17), we obtain

$$\text{Tr} [\overline{\rho}^2] \text{Tr} [\rho^2]^{-1} \leq \overline{\mathcal{L}(t)} \leq 1 - (\text{Tr} [\rho^2] - \text{Tr} [\overline{\rho}^2]). \quad (24)$$

This result says that the time-averaged Loschmidt echo is bounded from below by the ratio of the effective dimensions of the initial and equilibrium states and the difference from unity from above is given by at least the difference between initial and equilibrium purities. Note that in the limit of a *pure* (unity purity) initial state, both lower and upper bounds would be equal and we would recover the well-known result [36] $\overline{\mathcal{L}} = \text{Tr} [\overline{\rho}^2]$.

At this point, we can make a connection between the time-averaged Loschmidt echo and the bound on observable variances found by Reimann, Eq. (1). Since the upper bound is in terms of the purity of the time-averaged state (i.e. the time-averaged linearized echo), it is clear that the average Loschmidt echo need not be small to have good equilibration. Indeed, provided the initial purity $\text{Tr} [\rho(0)^2]$ is small enough, $\overline{\mathcal{L}}$ can be as close as we wish to unity. On the other hand, if $\overline{\mathcal{L}}$

is small, we are guaranteed that $\text{Tr} [\overline{\rho}^2]$ will be even smaller, since $\text{Tr} [\overline{\rho}^2] \leq \overline{\mathcal{L}}/d_{\text{eff}}$.

To find the short-time behavior of the Loschmidt echo, it is convenient to express the linearized echo as

$$\mathcal{L}_F(t) = \ll \rho | e^{-it\mathcal{H}} | \rho \gg, \quad (25)$$

where \mathcal{H} is a superoperator acting on elements of the Hilbert-Schmidt space as $\mathcal{H}\alpha = [H, \alpha]$. $|\rho\rangle\rangle$ is a ket in the Hilbert-Schmidt space, equivalent to the density operator ρ . Note, however, that this ket is not normalized with respect to the Hilbert-Schmidt norm, i.e. $\ll \rho | \rho \gg = \text{Tr} [\rho^2] = d_{\text{eff}}^{-1} \neq 1$ in general. Eq. (25) is the direct analog of the expression for the Loschmidt echo at zero temperature, $\mathcal{L}(t) = |\langle \Psi | e^{-itH} | \Psi \rangle|^2$.

The linearized echo can alternatively be expressed as the Fourier transform of the energy gap probability distribution $\chi(\omega) := \langle \delta(\omega - \mathcal{H}) \rangle = \ll \rho | \delta(\omega - \mathcal{H}) | \rho \gg$. Using this, in the same spirit as the analogous zero-temperature analysis [23] we consider the cumulant expansion of $\mathcal{L}_F(t)$

$$\mathcal{L}_F(t) = d_{\text{eff}}^{-1} \exp \left[\sum_{n=2}^{\infty} \frac{(-it)^n}{n!} \ll \mathcal{H}^n \gg_c \right], \quad (26)$$

where $\ll \mathcal{H}^n \gg_c$ represents the n -th cumulant of \mathcal{H} with respect to the state ρ and d_{eff}^{-1} is the normalization factor to ensure $\mathcal{L}_F(0) = \text{Tr} \rho^2$. The sum begins at $n = 2$ due to the cyclicity of the trace. The second cumulant is the variance of \mathcal{H} ,

$$\begin{aligned} \ll \mathcal{H}^2 \gg_c &= 2(\text{Tr} [\rho^2 H^2] - \text{Tr} [(\rho H)^2]) \\ &= 2\text{Tr} [\rho^2] \sum_{k>0} \frac{\text{Tr} [\rho_k^2 H_k^2] - \text{Tr} [(\rho_k H_k)^2]}{\text{Tr} [\rho_k^2] + 2}, \end{aligned}$$

and for short times, where only the second-order term contributes, we have

$$d_{\text{eff}} \mathcal{L}_F(t) \approx 1 - \frac{1}{2} \ll \mathcal{H}^2 \gg_c t^2. \quad (27)$$

Checking both this expansion and the short-time expansion of the exact Loschmidt echo (18), we find that in the off-critical region $1 - \mathcal{L}(t) \propto t^2 L$, a scaling that coincides with the zero-temperature result [23].

V. THE QUANTUM XY CHAIN

An important instance of the above class of quasi-free fermions (12) is the quantum XY chain in a transverse magnetic field,

$$H = - \sum_{i=1}^L \frac{(1+\gamma)}{2} \sigma_i^x \sigma_{i+1}^x + \frac{(1-\gamma)}{2} \sigma_i^y \sigma_{i+1}^y + h \sigma_i^z. \quad (28)$$

This is a well-known and long-studied model. A Jordan-Wigner mapping and Fourier transform bring the model to the form of Eq. (12), which allows for an exact solution [37, 38].

The XY chain (28) is of the same form as (12) with the identification $\epsilon_k = \cos(k) + h$ and $\Delta_k = \gamma \sin(k)$. The single-particle energies and the eigenstate-parametrizing angles are defined as previously: $\Lambda_k = \sqrt{\epsilon_k^2 + \Delta_k^2}$ and $\tan(\theta_k) = \frac{\Delta_k}{\epsilon_k}$. As is customary, we fix boundary conditions on the Fermi operators and choose anti-periodic ones [39, 40]. The momenta then take the values $k = (2n+1)\pi/L$, with $n = 0, \dots, L-1$.

This system exhibits two types of quantum critical lines at zero temperature: (i) the Ising transition for $|h| = 1$ and $\gamma \neq 0$, corresponding to a second-order quantum phase transition between ferromagnetic and paramagnetic phases, and (ii) the anisotropy transition for $\gamma = 0$ and $|h| < 1$, a second-order QPT between ferromagnetic phases with long-range order in the x or y directions for $\gamma > 0$ or $\gamma < 0$, respectively.

Here, we will explore in more detail the conditions for obtaining either of the two universal distributions for the LE (Log-Normal or double-peaked) for small quenches of the quantum XY chain.

In the following, we consider the logarithm of the LE, denoted by the quantity $\mathcal{Z}(t) = \ln \mathcal{L}(t)$. Expanding $\mathcal{Z}(t)$ up to second order in the quench amplitude, we obtain

$$\mathcal{Z}(t) = \overline{\mathcal{Z}} + \sum_{k>0} a_k \cos(\omega_k t), \quad (29)$$

where $a_k = (1 - c_k^{-1}) \sin^2(\Delta\theta_k)/2$ which at this order is equivalent to $a_k = (1 - c_k^{-1})(\Delta\theta_k)^2/2$ and $\omega_k = 2\Lambda_k^1$. Similarly, for the logarithm of the normalized and linearized quantity, $\mathcal{Z}_F(t) = \ln [d_{\text{eff}} \mathcal{L}(t)]$, we have

$$\mathcal{Z}_F(t) = \overline{\mathcal{Z}_F} + \sum_{k>0} a_k^F \cos(\omega_k t), \quad (30)$$

where $a_k^F = (1 - c_k^{-2})(\Delta\theta_k)^2/2$. From the very similar form of the coefficients a_k and a_k^F , we can see that both quantities will have qualitatively the same properties. If we now assume that the frequencies $\{\omega_k\}_{k>0}$ are rationally independent, the ergodic theorem implies that both $\mathcal{Z}(t)$ and $\mathcal{Z}_F(t)$ are given by a sum of independent random variables. The situation is perfectly analogous to that analyzed in Sec. III A (cfr. Eq. (10)) with the difference that Eqns. (29) and (30) represent a sum of $L/2$ independent variables as opposed to $D-1$ for Eq. (10). This is clearly due to the quasi-free character of the model.

As in the general case (cfr. Eq. (11)), rational independence allows to compute exactly the characteristic function of the centered variable $\mathcal{Z}(t) - \overline{\mathcal{Z}}$:

$$\overline{e^{i\lambda(\mathcal{Z}(t) - \overline{\mathcal{Z}})}} = \prod_{k>0} J_0(|\lambda a_k|). \quad (31)$$

All considerations given in Sec. III A carry over also in this case; however, knowledge of the precise analytical form of the weights a_k , a_k^F allows for a more detailed analysis.

The first result we recall here is that in the limit $L \rightarrow \infty$ the central limit theorem holds independently from other parameters such as quench amplitudes, temperature, and so on. In other words, when L is the largest length scale of the system (the off-critical region) the variable $(\mathcal{Z} - \overline{\mathcal{Z}})/\sqrt{L}$

tends in distribution to a Gaussian (the same result holds of course also for the linearized version). To show this, just note that since $0 \leq a_k, a_k^F \leq 1/2$, the total variance grows extensively in the whole parameter region. In fact, using $J_0(x) = 1 - x^2/4 + O(x^4)$, one obtains that the variance of \mathcal{Z} is $\kappa_2 = (1/2) \sum_{k>0} a_k^2$. Now, for L large one has: $\kappa_2 \simeq L/(4\pi) \int_0^\pi (a_k)^2 \leq L/8$ meaning that the variance always grows extensively with L . This in turns implies that, for $L \rightarrow \infty$, $(\mathcal{Z} - \overline{\mathcal{Z}})/\sqrt{L}$ is Gaussian-distributed with mean zero and variance $\sigma^2 = 1/(4\pi) \int_0^\pi (a_k)^2$. For the sake of the reader, we also compute the variance of \mathcal{L} in Appendix F.

On the other hand, let us now keep L finite and concentrate on the zero-temperature quasi-critical region, i.e. $T = 0$, $\xi \gg L$. As for general models, the weights a_k become highly peaked in the quasi-critical region, with very few dominating terms, so that Eqns. (29) and (30) correspond to a sum of few random variables, thus invalidating the conditions needed for the CLT to hold. This is clearly visible in Fig. 2, where we plot the coefficients a_k for small quenches close to the Ising and anisotropic critical lines. From Fig. 2, we can see the conditions in which few momenta contribute: sufficiently widely-spaced quasi-momenta, i.e. small-enough system size as compared to the width of the peak. As we will show explicitly, this corresponds to the quasi-critical region.

Let us now turn on the temperature. In the XY model considered here, $\zeta = \nu = 1$ for both kinds of transitions. According to the discussion in Sec. III C, the divergence of a_k at low energy is immediately suppressed for temperatures larger than the gap. Correspondingly, we expect a double-peaked distribution for \mathcal{Z} whenever the condition $T \ll \Delta$ is satisfied (the gap Δ is given in this case by the smallest ω_k). These general findings are confirmed by the explicit analysis of the temperature-dependent weights $a_k(T)$. Specifically $a_k(T) = d_{\omega_k}(T) a_k(T=0)$, where the temperature-damping factor $d_\omega(T) = 1 - \cosh(\omega/T)^{-m}$ ($m = 1, 2$ for the LE and linearized LE respectively). Since $d_{\omega_k}(T) \approx 1$ for $\Delta/T \gg 1$, the $T = 0$ behavior is recovered when $T \ll \Delta$. The expansion of $a_k(T)$ in the region $\Delta/T \ll 1$ confirms that the $T = 0$ divergence is suppressed. On the contrary, for large temperatures the effect of $d_\omega(T)$ is that of damping low-energy levels with respect to high-energy ones, resulting in more evenly-distributed weights a_k and making more pronounced the Gaussian behavior of \mathcal{Z} .

To summarize, the small-quench scenario is the following: i) quasi-critical, low temperature region $\xi \gg L$, $T \ll \Delta \Rightarrow$ few dominating weights $a_k \Rightarrow$ largely spread, double-peaked distribution for \mathcal{Z} ; ii) off-critical region, $L \gg \xi \Rightarrow$ large number of dominating weights $a_k \Rightarrow$ CLT and Gaussian behavior for \mathcal{Z} . An intermediate regime corresponds to an interpolation between these two limiting distributions (Gaussian and double-peaked).

The factor $\sin^2(\Delta\theta_k)$ may be written more-explicitly in terms of the Hamiltonian parameters as

$$\sin^2(\Delta\theta_k) = \frac{\sin^2(k)}{(\Lambda_k^0 \Lambda_k^1)^2} [(\gamma^1 - \gamma^0) \cos(k) + (\gamma^1 h^0 - \gamma^0 h^1)]^2 \quad (32)$$

Note that from this expression we can immediately observe

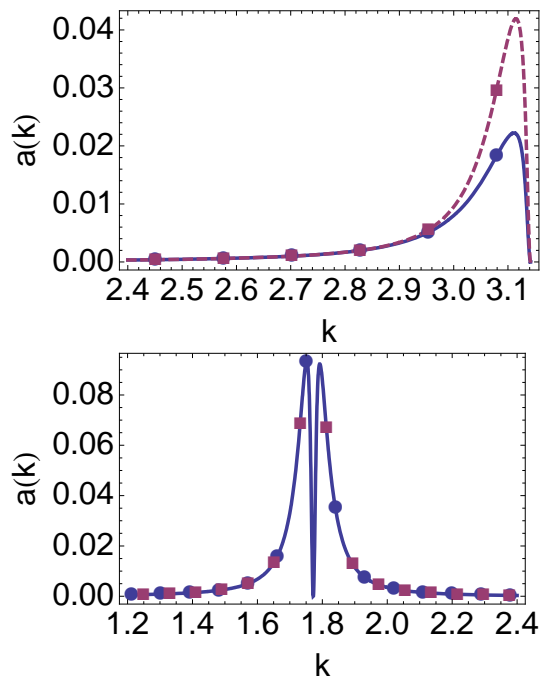


Figure 2: Top panel: a_k (solid) and a_k^F (dashed), for parameters $\gamma^{0,1} = 1$, $h^0 = 0.99$, $h^1 = 1.01$, $\beta = 16.67$ ($T = 0.06$). The dots and squares give the allowed quasi-momenta for $L = 50$. Bottom panel: a_k for near the anisotropy transition, with parameters $h^{0,1} = 0.2$, $\gamma^0 = 0.01$, $\gamma^1 = -0.01$, and $\beta = 40$ ($T = 0.025$). Circles show allowed weights for $L = 70$ while squares refer to $L = 78$. In the latter case two weights a_j have approximately the same value. This results in a single-peaked distribution function.

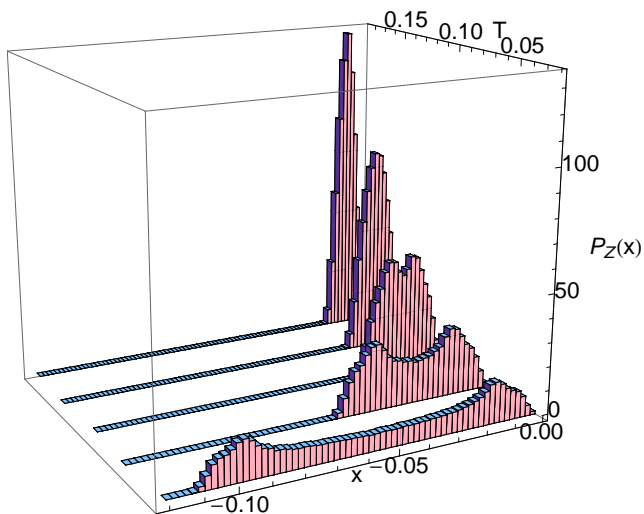


Figure 3: $P_Z(x)$ as the temperature is varied for a quench near the Ising transition. Notice how the double-peaked distribution becomes more Gaussian with an increase of temperature. Here, the temperature takes values $T = 0.02, 0.06, 0.1, 0.14, 0.18$ and the other parameters are $L = 50$, $h^0 = 0.99$, $h^1 = 1.01$, and $\gamma^{0,1} = 1$.

that the Loschmidt echo will be unity for any initial and final quench field h^0, h^1 of the isotropic ($\gamma = 0$) model. This follows from the fact that $[H_0, H_1] = 0$, provided $\gamma^0 = 0 = \gamma^1$. In the following we proceed to a detailed analysis of the $\sin^2(\Delta\theta_k)$ factor for small quenches close to both kinds of transition of the model, in order to characterize the number of terms contributing to the oscillatory part of Eqns. (29) and (30). This analysis closely mirrors that of Ref. [23].

A. Ising transition

Consider quenches near the Ising transition, taking $\gamma = 1$ with the difference $\delta h = h^1 - h^0$ assumed to be small. We first perform a change into energy variables, using Eq. (32),

$$\sin^2(\Delta\theta_k) = \frac{\sin^2(k)(h^1 - h^0)^2}{(\Lambda_k^0)^2(\Lambda_k^1)^2} \quad (33)$$

$$\approx \frac{(\omega^2 - E_m^2)(E_M^2 - \omega^2)\delta h^2}{4(h^0)^2\omega^4} \quad (34)$$

$$= c(\omega) \quad (35)$$

where $\omega = \Lambda_k^{(0)}$, $E_m = |1 - h^0|$, and $E_M = |1 + h^0|$.

As also shown in [23], $c(\omega)$ is a bell-shaped function. The number of momenta that are included in the peak determines how many oscillatory terms contribute to $\mathcal{Z}(t)$, and hence the shape of the distribution $P_Z(x)$. Notice, importantly, that the shape of the multiplicative factor $(1 - c_k^{-m})$ ($m = 1, 2$ for LE and linearized LE, respectively) serves *only* to weight less-strongly the lower-energy modes. In other words, it appears that increasing temperature will never concentrate the spectral weights, but will rather tend to make the distribution more approximately Gaussian due to the enhanced relative weights of the higher-energy modes.

The width of the peak δc of $c(\omega)$, estimated by the inflection point, is approximately $\delta c \approx 1.8|1 - h^0|$ [42][23]. In order for the temperature-dependent pre-factor $d_\omega(T)$ to not smear out the weights towards large frequencies, the region for which $d_\omega(T)$ is small must be smaller than δc . That is, provided the quench parameters are those that would produce a double-peaked distribution in the $T = 0$ case, in order to get a double-peaked distribution at finite temperature we need $|1 - h^0|\beta \gg 1$, that is $T \ll \Delta$ (Δ , the gap, is $|1 - h^0|$ for $\gamma = 1$).

To check this analysis, let's take a look at the following example. Let $L = 50$, $h^0 = 0.99$, $h^1 = 1.01$ and $\gamma^0 = \gamma^1 = 1$. In this case, $L \ll |h - 1|^{-1}$, so we expect to see a double-peaked shape in the $T = 0$ limit. This is certainly the case, and the distribution has been plotted in Fig. 3. As the temperature is increased, the double peak begins to become less evident between $T = 0.1$ and $T = 0.14$. As T increases through this range, the condition $1/\beta \gg |h - 1|$ begins to hold and $P_Z(x)$ becomes more nearly Gaussian.

B. Anisotropy transition

The procedure for examining $P_{\mathcal{Z}}(x)$ in the vicinity of the anisotropy transition goes much the same as for the Ising transition. The only extra complication here is due to the form of the single-particle energy, as it is not one-to-one with the momentum and does not allow an immediate change from momentum to energy variables over the whole range of possible momenta. Consider the simple case $h^1 = h^0$, such that we quench only via the anisotropy parameter. In the following we consider the case $h = 0$, where the minimum of the single-particle energy is obtained for $k_F = \pi/2$ and the gap is simply given by $\Delta = |\gamma|$. For other values of the magnetic field h , the location of the Fermi momentum will shift but the following analysis will be qualitatively similar. Though $k \rightarrow \Lambda_k$ is not 1-1, let us restrict ourselves to the interval $k \in [\pi/2, \pi]$, in which the map is indeed 1-1. In this case, define

$$c_a(\omega_0, \omega_1) = \frac{(1 - \omega_0^2)(\omega_0^2 - (\gamma^0)^2)}{(1 - (\gamma^0)^2)(\omega_0\omega_1)^2} (\gamma^1 - \gamma^0)^2 \quad (36)$$

as the function corresponding to $c(\omega)$ for the Ising model case. Taking $|\delta\gamma| \ll 1$ and expanding in $\delta\gamma$ to second-order, we obtain

$$c_a(\omega) = \frac{(1 - \omega^2)(\omega^2 - (\gamma^0)^2)}{(1 - (\gamma^0)^2)\omega^4} (\delta\gamma)^2. \quad (37)$$

Just as in the Ising case, this function is bell-shaped. The width of $c_a(\omega)$ as given by the location of the inflection point is approximately $\delta c_a \approx 1.8 |\gamma^0|$. Exactly as found near the Ising transition, the temperature factor suppresses the peak of the $\sin^2(\Delta\theta)$, broadening the number of momenta which contribute appreciably to the sums (29) and (30). Consequently, in addition to the $T = 0$ requirements for obtaining a double-peaked distribution, we must require that $1/\beta \ll |\gamma^0|$, i.e. $T \ll \Delta$. One notable difference between the statistics for quenches near the anisotropy versus Ising transition is the potential for obtaining a single-peaked distribution such as is shown in Fig. 4, directly analogous to the single-particle DOS of a two-dimensional isotropic tight-binding model. This phenomenon is due to the band structure near the anisotropy transition in which the Fermi momentum is at an intermediate (incommensurate) value of $k \in [0, \pi]$ rather than at the edge, as it is near the Ising transition. Consequently, the weights a_k have a double-peaked form, as shown in the bottom panel of Fig. 2. For certain system sizes, then, it is possible that the quasi-momenta will be approximately symmetrically placed about the Fermi momentum, resulting in the weights a_k appearing in pairs (see e.g. the $L = 78$ example in the bottom panel of Fig. 2). In the quasi-critical regime, since the separation between peaks of the double-peaked distribution for $P_{\mathcal{Z}}(x)$ is proportional to the difference between the two largest weights (peaks of $P_{\mathcal{Z}}(x)$ are at $\bar{\mathcal{Z}} \pm |a_1 - a_2|$, where $a_{1,2}$ are the two largest weights [23]), if the two maximal weights are nearly equal the peaks will appear merged. However, this distribution is to be understood as simply a special case of the usual double-peaked behavior we have observed

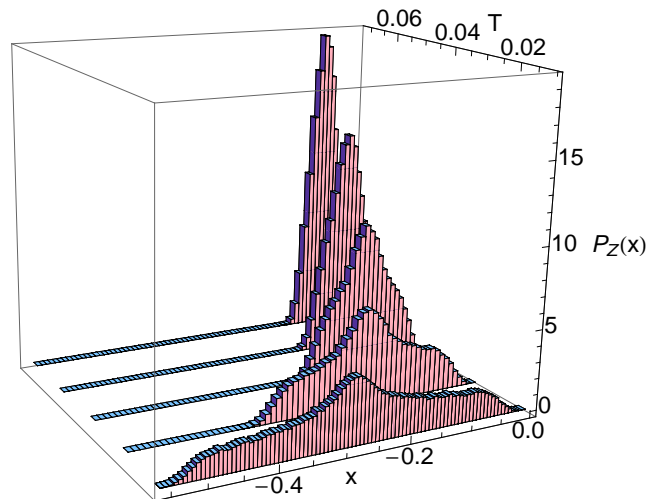


Figure 4: $P_{\mathcal{Z}}(x)$ as the temperature is varied for a quench near the anisotropy transition. Notice how the single-peaked distribution becomes more Gaussian with an increase of temperature. Here, the temperature takes values $T = 0.01, 0.025, 0.04, 0.055, 0.07$ and the other parameters are $L = 78$, $h^{0,1} = 0.2$, $\gamma^0 = 0.01$, and $\gamma^1 = -0.01$.

for the Ising case. Indeed, if we were to take the same set of parameters for the above example but a slightly different system size (e.g. $L = 70$), we will obtain the same type of double-peaked distribution as we have seen in Fig. 3. We remark that the $h^{0,1} = 0$ case we have considered in the preceding analysis is slightly pathological, in that due to the Fermi momentum appearing at exactly $k_F = \pi/2$, all weights a_k will come in pairs. However, for non-zero magnetic fields we find that in the overwhelming majority of cases we will find a double-peaked distribution as the quasi-momenta corresponding to the maximal pair of weights will normally not be very symmetrically-displaced about the Fermi level.

VI. CONCLUSION

In this paper we have studied the problem of the long-time out-of-equilibrium dynamics of a quantum system after a Hamiltonian quench of a thermal (Gibbs) state. More specifically, we have examined the infinite-time statistics of the thermal Loschmidt echo \mathcal{L} [25]. This latter is a global quantity that depends just on the Hamiltonian and on the initial state, i.e. no preferred observable has to be singled out, and bears relevance for the general quantum equilibration problem. \mathcal{L} can be naturally defined as the Uhlmann fidelity between the initial finite-temperature Gibbs state associated with a Hamiltonian and the time-dependent one obtained by the unitary evolution corresponding to a different (quenched) Hamiltonian.

For a small quench we argued, on fairly general grounds, that a Log-Normal distribution $P_{\mathcal{L}}$ is realized for off-critical

systems at arbitrary temperatures. On the other hand, if the quantum quench is performed near a quantum critical point a dramatically different scenario emerges. For sufficiently small temperatures a universal double-peaked distribution isomorphic to the DOS of a two-dimensional tight-binding model is realized. As the temperature increases this singular distribution can either be continuously morphed into the former Log-Normal distribution or not depending on whether or not the quench enacts a sufficiently irrelevant perturbation.

In the second part of the paper we applied the above general analysis to the paradigmatic case of a finite-temperature quantum XY chain in a transverse magnetic field. In this case a plethora of analytical results can be obtained for ar-

bitrarily large quenches, far or close to the critical lines of the model. In particular, we have found a tight lower bound on the Loschmidt echo for a class of XY-type models in terms of a simplified “linearized” Loschmidt echo.

The extension of this long-time probability distribution approach to general physically relevant observables appears as a compelling task for future investigations.

Acknowledgments- We acknowledge useful discussions with Siddhartha Santra. NTJ is grateful for support from an Oakley Fellowship, LCV acknowledges support from European project COQUIT under FET-Open grant number 2333747, and PZ acknowledges support from NSF grants PHY-803304, PHY-0969969, and DMR-0804914.

-
- [1] P. Calabrese and J. Cardy, Phys. Rev. Lett. **96**, 136801 (2006).
 [2] M. A. Cazalilla, Phys. Rev. Lett. **97** (2006).
 [3] S. R. Manmana, S. Wessel, R. M. Noack, and A. Muramatsu, Phys. Rev. Lett. **98**, 210405 (2007).
 [4] A. Silva, Phys. Rev. Lett. **101**, 120603 (2008).
 [5] J. von Neumann, Zeit. Für Phys. **57**, 30 (1929), see also the English translation: Eur. Phys. J. H, **35**, 201 (2010).
 [6] H. Tasaki, Phys. Rev. Lett. **80**, 1373 (1998).
 [7] S. Goldstein, J. L. Lebowitz, R. Tumulka, and N. Zanghì, Phys. Rev. Lett. **96**, 050403 (2006).
 [8] P. Reimann, Phys. Rev. Lett. **99**, 160404 (2007).
 [9] P. Reimann, Phys. Rev. Lett. **101**, 190403 (2008).
 [10] N. Linden, S. Popescu, A. J. Short, and A. Winter, Phys. Rev. E **79**, 061103 (2009).
 [11] A. Riera, C. Gogolin, and J. Eisert, arXiv:1102.2389 (2011).
 [12] C. Gogolin, M. Mueller, and J. Eisert, Phys. Rev. Lett. **106**, 040401 (2011).
 [13] S. Trotzky, Y.-A. Chen, A. Flesch, I. McCulloch, U. Schollwöck, J. Eisert, and I. Bloch, arXiv:1101.2659.
 [14] A. Peres, Phys. Rev. A **30**, 1610 (1984).
 [15] T. Gorin, T. Prosen, T. Seligman, and M. Žnidarič, Phys. Rep. **435**, 33 (2006).
 [16] N. T. Jacobson, P. Giorda, and P. Zanardi, Phys. Rev. E **82**, 056204 (2010).
 [17] D. Rossini, T. Calarco, V. Giovannetti, S. Montangero, and R. Fazio, J. Phys. A: Math. Theor. **40**, 8033 (2007).
 [18] D. Rossini, T. Calarco, V. Giovannetti, S. Montangero, and R. Fazio, Phys. Rev. A **75**, 032333 (2007).
 [19] H. T. Quan, Z. Song, X. F. Liu, P. Zanardi, and C. P. Sun, Phys. Rev. Lett. **96**, 140604 (2006).
 [20] T. Gorin, T. Prosen, T. H. Seligman, and W. T. Strunz, Phys. Rev. A **70**, 042105 (2004).
 [21] M. Žnidarič and T. Prosen, J. Phys. A: Math. Gen. **36**, 2463 (2003).
 [22] P. Zanardi, H. T. Quan, X. Wang, and C. P. Sun, Phys. Rev. A **75**, 032109 (2007).
 [23] L. Campos Venuti and P. Zanardi, Phys. Rev. A **81**, 022113 (2010).
 [24] L. Campos Venuti and P. Zanardi, Phys. Rev. A **81**, 032113 (2010).
 [25] L. Campos Venuti, N. T. Jacobson, S. Santra, and P. Zanardi, arXiv:1104.3232 (2011).
 [26] N. Linden, S. Popescu, A. J. Short, and A. Winter, Phys. Rev. E **79**, 061103 (2009).
 [27] A. Uhlmann, Rep. Math. Phys. **9**, 273 (1976).
 [28] J. Miszczyk, Z. Puchała, P. Horodecki, A. Uhlmann, and K. Życzkowski, Quant. Inf. and Comp. **9**, 0103 (2009).
 [29] M. Hübner, Phys. Lett. A **163**, 239 (1992).
 [30] H.-J. Sommers and K. Życzkowski, J. Phys. A: Math. Gen. **36**, 10083 (2003).
 [31] P. Zanardi, L. Campos Venuti, and P. Giorda, Phys. Rev. A **76**, 062318 (2007).
 [32] C. De Grandi, V. Gritsev, and A. Polkovnikov, Phys. Rev. B **81**, 224301 (2010).
 [33] C. De Grandi, V. Gritsev, and A. Polkovnikov, Phys. Rev. B **81**, 012303 (2010).
 [34] L. Campos Venuti and P. Zanardi, Phys. Rev. Lett. **99**, 095701 (2007).
 [35] J. Häppölä, G. Halász, and A. Hamma (2010), arXiv:1011.0380.
 [36] L. Campos Venuti and P. Zanardi, Phys. Rev. A **81**, 022113 (2010).
 [37] E. Lieb, T. Schultz, and D. Mattis, Ann. Phys. (New York) **16**, 407 (1961).
 [38] P. Pfeuty, Ann. Phys. (New York) **57**, 79 (1970).
 [39] E. Lieb, T. Schultz, and D. Mattis, Ann. of Phys. **16**, 407 (1961).
 [40] E. Barouch, B. M. McCoy, and M. Dresden, Phys. Rev. A **2**, 1075 (1970).
 [41] In most cases this seems to be a plausible assumption, see note [13] of Ref. [25].
 [42] Note the different convention for Λ_k used here, as one-half that of Ref. [23].

Appendix A: Proof of the qubit inequality

We prove here the following inequality for arbitrary single-qubit states ρ and unitary operators U ,

$$\frac{\text{Tr} [U\rho U^\dagger \rho]}{\text{Tr} [\rho^2]} \leq \text{Tr} \left[\sqrt{\rho^{\frac{1}{2}} U \rho U^\dagger \rho^{\frac{1}{2}}} \right]^2. \quad (\text{A1})$$

Expressing ρ in Bloch form, $\rho = \frac{1}{2}(\mathbb{I} + \vec{v} \cdot \vec{\sigma})$, we have

$$\begin{aligned} \text{Tr} [\rho_0 \rho_1] &= \frac{1}{2}(1 + \vec{v}_0 \cdot \vec{v}_1), \\ \det [\rho] &= \frac{1}{4}(1 - v^2). \end{aligned}$$

As shown by Hübner [29], the Uhlmann fidelity between arbitrary single-qubit states ρ and σ is

$$\mathrm{Tr} \left[\sqrt{\rho^{\frac{1}{2}} \sigma \rho^{\frac{1}{2}}} \right]^2 = \mathrm{Tr} [\rho \sigma] + 2\sqrt{\det [\rho] \det [\sigma]}.$$

Using this and the fact that a unitary transformation leaves the magnitude of the Bloch vector unchanged, define $v = |v_{0,1}|$, $\vec{v}_0 \cdot \vec{v}_1 = v^2 \cos \theta$, and

$$\begin{aligned} \text{RHS} &= \mathrm{Tr} [\rho^2] \mathrm{Tr} \left[\sqrt{\rho^{\frac{1}{2}} U \rho U^\dagger \rho^{\frac{1}{2}}} \right]^2 \\ &= \frac{1}{2}(1+v^2) \left[\frac{1}{2}(1+v^2 \cos \theta) + \frac{1}{2}(1-v^2) \right], \\ \text{LHS} &= \mathrm{Tr} [U \rho U^\dagger \rho] \\ &= \frac{1}{2}(1+v^2 \cos \theta). \end{aligned}$$

Finally,

$$\begin{aligned} 4(\text{RHS} - \text{LHS}) &= v^2(1 - \cos \theta) - v^4(1 - \cos \theta) \\ &= v^2(1 - \cos \theta)(1 - v^2) \\ &\geq 0, \end{aligned}$$

since $0 \leq v^2 \leq 1$.

Appendix B: Proof of the bound for quasi-free fermions

We now prove that the inequality (14) holds for Gibbs states of quasi-free fermions of the form Eq. (12):

$$\frac{\mathrm{Tr}(U \rho U^\dagger \rho)}{\mathrm{Tr}(\rho^2)} \leq \left[\mathrm{Tr} \sqrt{\rho^{\frac{1}{2}} U \rho U^\dagger \rho^{\frac{1}{2}}} \right]^2 \quad (\text{B1})$$

Exploiting the tensor-product form for the Gibbs state

$$\rho^\alpha = \frac{e^{-\beta H_\alpha}}{Z_\alpha} = \bigotimes_{k>0} \frac{1}{Z_k^\alpha} [\rho_k^\alpha \oplus \mathbb{I}_k],$$

where [22]

$$\begin{aligned} J_k^\alpha &:= \cos(\theta_k^\alpha) \sigma_k^z + \sin(\theta_k^\alpha) \sigma_k^y \\ \rho_k^\alpha &:= \exp(-\beta \Lambda_k^\alpha J_k^\alpha) = \cosh(\beta \Lambda_k^\alpha) \mathbb{I} - \sinh(\beta \Lambda_k^\alpha) J_k^\alpha \end{aligned}$$

we can straightforwardly compute

$$\begin{aligned} \mathrm{Tr} [U \rho U^\dagger \rho] &= \prod_{k>0} \frac{1}{Z_k^2} \left[\mathrm{Tr} [U_k \rho_k U_k^\dagger \rho_k] + 2 \right], \\ \mathrm{Tr} [\rho^2] &= \prod_{k>0} \frac{1}{Z_k^2} \left[\mathrm{Tr} [\rho_k^2] + 2 \right], \\ \mathrm{Tr} \left[\sqrt{\rho^{\frac{1}{2}} U \rho U^\dagger \rho^{\frac{1}{2}}} \right]^2 &= \prod_{k>0} \frac{1}{Z_k^2} \left[\mathrm{Tr} \left[\sqrt{\rho_k^{\frac{1}{2}} U_k \rho_k U_k^\dagger \rho_k^{\frac{1}{2}}} \right] + 2 \right]^2. \end{aligned}$$

Note that $Z_k = 2(1 + \cosh(\beta \Lambda_k))$, so $4 \leq Z_k < \infty$. For the following, define $x := \beta \Lambda_k^0$ and $v := \sin^2(\beta \Lambda_k^1 t)(1 -$

$\cos(2\Delta\theta_k))$, where $0 \leq v \leq 2$. We also make use of the following:

$$\begin{aligned} \mathrm{Tr} [U_k \rho_k U_k^\dagger \rho_k] &= 2 \cosh(2x) - 2 \sinh^2(x)v, \\ \mathrm{Tr} [\rho_k^2] &= 2 \cosh(2x), \\ \mathrm{Tr} \left[\sqrt{\rho_k^{\frac{1}{2}} U_k \rho_k U_k^\dagger \rho_k^{\frac{1}{2}}} \right]^2 &= 2 [2 \cosh^2(x) - \sinh^2(x)v] \end{aligned}$$

Defining $f(x, v) := 2 \cosh^2(x) - \sinh^2(x)v$, we have

$$\begin{aligned} \mathrm{Tr} [U_k \rho_k U_k^\dagger \rho_k] &= 2(f(x, v) - 1), \\ \mathrm{Tr} \left[\sqrt{\rho_k^{\frac{1}{2}} U_k \rho_k U_k^\dagger \rho_k^{\frac{1}{2}}} \right]^2 &= 2f(x, v). \end{aligned}$$

Now, taking only the k^{th} term of the products above, in order to prove the validity of (B1) we need to check whether the quantity

$$\begin{aligned} Q(x, v) &:= \frac{1}{Z_k^2} \left[\mathrm{Tr} [\rho_k^2] + 2 \right] \left[\mathrm{Tr} \left[\sqrt{\rho_k^{\frac{1}{2}} U_k \rho_k U_k^\dagger \rho_k^{\frac{1}{2}}} \right] + 2 \right]^2 \\ &\quad - \left[\mathrm{Tr} [U_k \rho_k U_k^\dagger \rho_k] + 2 \right] \end{aligned}$$

is non-negative. Re-writing in terms of $f(x, v)$, as above, we have

$$Q(x, v) = \frac{\cosh(2x) + 1}{2(1 + \cosh(x))^2} \left(\sqrt{2f(x, v)} + 2 \right)^2 - 2f(x, v).$$

Consider

$$\begin{aligned} \partial_v Q(x, v) &= \frac{-\cosh(2x) + 1}{(1 + \cosh(x))^2} \sinh^2(x) \left[1 + \frac{\sqrt{2}}{2\sqrt{f(x, v)}} \right] \\ &\quad + 2 \sinh^2(x), \end{aligned}$$

and

$$\begin{aligned} \partial_v^2 Q(x, v) &= \frac{-\sqrt{2}(\cosh(2x) + 1) \sinh^4(x)}{2(1 + \cosh(x))^2} \left(f(x, v) \right)^{-3/2} \\ &\leq 0. \end{aligned}$$

Since the concavity of $Q(x, v)$ with respect to v is never positive, to minimize it we need only consider the boundaries, $v = 0, 2$. We find that $Q(x, 0) = 0$ and $Q(x, 2) \geq 0 \forall x$, and hence have shown that $Q(x, v) \geq 0 \forall (x, v)$. The inequality (B1) follows.

Appendix C: Effective dimension d_{eff}

The effective dimension is defined to be the reciprocal of the purity, $d_{\text{eff}} = \mathrm{Tr} [\rho^2]^{-1}$. Now, the purity of the Gibbs

state (13) is simply

$$\begin{aligned}
\text{Tr} [\rho^2] &= \text{Tr} \left[\bigotimes_{k>0} \frac{1}{Z_k^2} [\rho_k^2 \oplus \mathbb{I}_k] \right] \\
&= \prod_{k>0} \frac{1}{Z_k^2} (\text{Tr} [\rho_k^2] + 2) \\
&= \prod_{k>0} \frac{2 + 2 \cosh(2\beta\Lambda_k)}{4(1 + \cosh(\beta\Lambda_k))^2} \\
&= \prod_{k>0} \left(\frac{\cosh(\beta\Lambda_k)}{1 + \cosh(\beta\Lambda_k)} \right)^2.
\end{aligned}$$

Appendix D: Linearized Loschmidt echo $\mathcal{L}_F(t)$

The ‘‘linearized’’ Loschmidt echo is defined to be

$$\begin{aligned}
\mathcal{L}_F(t) &= \text{Tr} [\rho(t)\rho] \\
&= \text{Tr} \left[\bigotimes_{k>0} \frac{1}{(Z_k^0)^2} \left[e^{-itH_k^1} e^{-\beta H_k^0} e^{itH_k^1} e^{-\beta H_k^0} \oplus \mathbb{I}_k \right] \right] \\
&= \prod_{k>0} \frac{1}{(Z_k^0)^2} \left[2 + \text{Tr} \left[e^{-itH_k^1} e^{-\beta H_k^0} e^{itH_k^1} e^{-\beta H_k^0} \right] \right],
\end{aligned}$$

where $H_k^{0,1}$ are the Hamiltonian operators on the even subspace of the k^{th} momentum subsystem (See [22]). Now, to evaluate the trace inside the product, we need the following [22]:

$$\begin{aligned}
e^{-itH_k^1} &= \cos(\Lambda_k^1 t) - i \sin(\Lambda_k^1 t) J_k^1 \\
e^{-\beta H_k^0} &= \cosh(\beta\Lambda_k^0) - \sinh(\beta\Lambda_k^0) J_k^0,
\end{aligned}$$

and

$$\begin{aligned}
\text{Tr} [J_k^0 J_k^1] &= 2 \cos(\theta_k^0 - \theta_k^1) \\
\text{Tr} [(J_k^1 J_k^0)^2] &= 2 \cos(2(\theta_k^0 - \theta_k^1))
\end{aligned}$$

After some algebra, we have

$$\begin{aligned}
\mathcal{L}_F(t) &= \prod_{k>0} \left[\left(\frac{\cosh(\beta\Lambda_k^0)}{1 + \cosh(\beta\Lambda_k^0)} \right)^2 \right. \\
&\quad \left. - \left(\frac{\cosh(\beta\Lambda_k^0) - 1}{\cosh(\beta\Lambda_k^0) + 1} \right) \sin^2(\Delta\theta_k) \sin^2(\Lambda_k^1 t) \right] \\
&= \text{Tr} [\rho^2] \prod_{k>0} \left[1 - \left(1 - \frac{1}{\cosh^2(\beta\Lambda_k^0)} \right) \times \right. \\
&\quad \left. \sin^2(\Delta\theta_k) \sin^2(\Lambda_k^1 t) \right]
\end{aligned}$$

The time average $\overline{\mathcal{L}_F}$ can be straightforwardly calculated by exploiting the rational independence of the single-particle energies.

Appendix E: Time-average, $\overline{\mathcal{L}}$

To compute the time average, re-group the product in the expression (18) for the Loschmidt echo into a sum:

$$\mathcal{L}(t) = 1 + \sum_{k>0} X_k(t) + \sum_{k_1>k_2>0} X_{k_1}(t) X_{k_2}(t) + \dots$$

where

$$X_k(t) = \sum_{m=1}^{\infty} h_k^{(m)} \sin^{2m}(\Lambda_k^1 t)$$

and

$$h_k^{(m)} := \begin{cases} \frac{c_k b_k}{1+c_k}, & m=1 \\ \frac{2c_k}{(1+c_k)^2} (b_k)^m \binom{1/2}{m}, & m>1 \end{cases}$$

Note that

$$\overline{\sin^{2m}(x)} = 2^{-2m} \binom{2m}{m} = (-1)^m \binom{-1/2}{m}.$$

Making use of the rational independence of the single-particle energies $\{\Lambda_k\}_{k>0}$ and regrouping into a product, we obtain

$$\overline{\mathcal{L}} = \prod_{k>0} \left(1 + G_k^{(1)} \right),$$

with

$$\begin{aligned}
G_k^{(1)} &= \sum_{m=1}^{\infty} h_k^{(m)} (-1)^m \binom{-1/2}{m} \\
&= \frac{c_k b_k}{2(1+c_k)} + \frac{2c_k}{(1+c_k)^2} \left[\frac{2}{\pi} \text{E}(-b_k) - \frac{b_k}{4} - 1 \right],
\end{aligned}$$

where

$$\begin{aligned}
c_k &:= \cosh(\beta\Lambda_k^0) \\
b_k &:= -(1 - c_k^{-2}) \sin^2(\Delta\theta_k)
\end{aligned}$$

and $\text{E}(x)$ is the complete elliptic integral.

Appendix F: Variance of \mathcal{L}

For completeness we sketch here the procedure to compute the variances. Squaring Eq. (18), regrouping the product into a sum, and taking the time average in exactly the same way as we did for the mean, we obtain

$$\overline{\mathcal{L}^2} = \prod_{k>0} \left(1 + G_k^{(2)} \right), \quad (\text{F1})$$

where

$$G_k^{(2)} = \sum_{m=1}^{\infty} g_k^{(m)} (-1)^m \binom{-1/2}{m} \quad (\text{F2})$$

and

$$g_k^{(m)} = 2h_k^{(m)} + \sum_{n=1}^{m-1} h_k^{(n)} h_k^{(m-n)}. \quad (\text{F3})$$

We now consider small quenches, expanding $\Delta^2 \mathcal{L} := \overline{\mathcal{L}^2} - (\overline{\mathcal{L}})^2$ to lowest order in $\Delta\theta_k$ with *fixed* system size L . (The determination of whether the quench is “large” or “small” must be made with respect to the system size). Expanding the square mean and the mean-squared terms into sums,

$$\begin{aligned} \overline{\mathcal{L}^2} &= 1 + \sum_{k>0} G_k^{(2)} + \sum_{k_1>k_2>0} G_{k_1}^{(2)} G_{k_2}^{(2)} + \dots \\ (\overline{\mathcal{L}})^2 &= 1 + \sum_{k>0} \left(2G_k^{(1)} + (G_k^{(1)})^2 \right) \\ &\quad + 4 \sum_{k_1>k_2>0} G_{k_1}^{(1)} G_{k_2}^{(1)} + \dots \end{aligned}$$

Only the lowest non-zero power of $\Delta\theta_k$ is to be retained, which turns out to be the fourth-order term. We find,

$$\begin{aligned} \Delta^2 \mathcal{L} &\approx \sum_{k>0} \left(G_k^{(2)} - 2G_k^{(1)} - (G_k^{(1)})^2 \right) \\ &\quad + \sum_{k_1>k_2>0} G_{k_1}^{(2)} G_{k_2}^{(2)} - 4G_{k_1}^{(1)} G_{k_2}^{(1)} \\ &\approx \frac{1}{8} \sum_{k>0} \left(1 - \frac{1}{\cosh(\beta\Lambda_k^0)} \right)^2 (\Delta\theta_k)^4. \end{aligned}$$

We can see from this expression how increasing the temperature (lowering β) tends to decrease the variance, while if the angle differences $\Delta\theta_k$ are large (as occurs for even small quenches near a critical point), the variance becomes larger. Note that here we have fixed L , so this small-quench expansion does not provide information on the finite-size scaling of the variance. Since each term in the products defining $\overline{\mathcal{L}^2}$ and $(\overline{\mathcal{L}})^2$ is smaller than unity, generically each of these products will vanish exponentially as a function of L . Hence, since the variance is a difference of two exponentially small functions we expect the variance to vanish exponentially with L as well.